Magneto–Tectonic Displacement Events (MTDE): A Threshold Framework for Rotational Instability and Earth-System Reorganization

Craig Stone

March 8, 2026

1 Plain Language Summary

For more than a century, paleomagnetic observations have provided a unique window into the relationship between Earth's magnetic field, planetary rotation, and the motion of the solid Earth. When rocks form, magnetic minerals within them align with the geomagnetic field, preserving a record of the field's direction at that moment in time. By measuring these preserved directions in rocks of different ages, scientists can reconstruct the past positions of the magnetic pole and track how it appears to move relative to the Earth's surface. Runcorn emphasized that paleomagnetism effectively measures the orientation of a vector fixed within the Earth relative to the planet's rotation axis, providing a geological record of planetary-scale motion unobservable directly through astronomy [Runcorn, 1968].

Theoretical work soon showed that such reorientation is physically expected for a rotating planet. Goldreich and Toomre demonstrated that redistribution of mass within the Earth—arising from mantle convection, density heterogeneity, or tectonic reorganization—changes the planet's inertia tensor and can cause the rotation axis to shift relative to the solid Earth [Goldreich and Toomre, 1969]. In this framework, polar wandering emerges naturally from the physics of rotating bodies: when internal mass distributions evolve, the planet adjusts its orientation in order to maintain rotational stability.

Recent synthesis has strengthened this interpretation by placing true polar wander within the broader dynamics of the Earth system. [Wang and Mitchell, 2023] review geological, geodynamic, and paleomagnetic evidence demonstrating that planetary reorientation is a fundamental consequence of mass redistribution within the mantle and lithosphere. Their work emphasizes that true polar wander should not be regarded as a rare or speculative process, but rather as an integral component of planetary evolution linking mantle convection, tectonic reorganization, climate change, and biological evolution across geological time. In this view, polar motion reflects the continual adjustment of the Earth system toward rotational equilibrium as its internal structure evolves. Within the paleomagnetic record, one of the most striking manifestations of geomagnetic variability is the occurrence of short-lived geomagnetic excursions. During these events, the direction of the magnetic field departs dramatically from the geographic poles and the field intensity weakens substantially, before the dipole field rapidly recovers. High-resolution sedimentary and volcanic records demonstrate that such excursions occur globally and typically persist for only a few thousand years [Channell et al., 2020]. These events therefore represent brief intervals during which the geomagnetic field temporarily loses its usual stability.

The MTDE framework builds on this historical foundation by approaching geomagnetic excursions from a dynamical-systems perspective. Rather than interpreting excursions solely as stochastic fluctuations of the geodynamo, we reconstruct geomagnetic pole motion as the trajectory of a nonlinear dynamical system. The results suggest that excursions arise when the Earth system approaches a stability boundary within a coupled rotational–magnetic phase space defined by torque and inertia. In this interpretation, the excursion record does not merely document irregular disturbances of the magnetic field; it provides a diagnostic of the stability structure of the coupled rotational and geomagnetic dynamics of the Earth system.

Abstract

Large-scale reorganizations of the Earth system—true polar wander episodes, geomagnetic excursions, large igneous province emplacement, and abrupt global climate perturbations—are commonly treated as distinct phenomena. Here we explore the possibility that a subset of these events may arise from a shared dynamical mechanism: transient threshold exceedance in a weakly coupled torque–inertia system.

We formalize this mechanism as a Magneto–Tectonic Displacement Event (MTDE), defined by the temporal coincidence of elevated inertia forcing (dI/dt) and magnetic torque forcing (dB/dt) exceeding a rotational stability boundary.

The framework is developed in mechanical terms, constrained by angular momentum conservation and inertia tensor evolution. We examine its applicability to large igneous province emplacement, geomagnetic instability intervals, and statistically anomalous climate events. The Paleocene–Eocene Thermal Maximum (PETM) is evaluated as a structured test case rather than an illustrative analogy.

The MTDE hypothesis is advanced as a falsifiable dynamical framework: it predicts specific alignments among mantle mass redistribution, paleomagnetic instability, and climate amplification processes. Its validity rests not on narrative coherence but on whether the torque–inertia phase space admits instability under empirically constrained forcing magnitudes.

2 Introduction

Earth history exhibits episodic intervals of rapid planetary-scale reorganization. These episodes appear across multiple observational domains: paleomagnetic instability, abrupt climatic excursions, large igneous province emplacement, oceanic anoxia, and sudden biospheric turnover.

Conventional interpretations treat these phenomena largely independently, assigning them to separate causal mechanisms operating within different subsystems of the Earth. Volcanic outpourings are attributed to mantle plume dynamics; geomagnetic excursions are interpreted as stochastic fluctuations of the geodynamo; climate perturbations are often attributed to carbon cycle feedbacks.

While these explanations may be individually plausible, they do not address a broader empirical question: why do these phenomena appear to cluster in time and, in some cases, exhibit coherent spatial structure?

The possibility that these apparently disparate phenomena arise from a common dynamical mechanism has been explored intermittently in the literature. Early mechanical treatments of planetary rotation emphasized the sensitivity of rotating bodies to changes in inertia distribution [Gold, 1955, Munk and MacDonald, 1960]. Subsequent work on true polar wander demonstrated that redistribution of mantle mass can alter the orientation of the Earth's principal inertia axes relative to the rotation vector [Tsai and Stevenson, 1972, Matsuyama and Nimmo, 2006].

At the same time, studies of geomagnetic excursions reveal that the geodynamo periodically enters unstable regimes in which the dipole field weakens and the virtual geomagnetic pole migrates rapidly across the globe [Valet and Fournier, 2012, Lund and Stoner, 2015].

These observations suggest that the rotational and magnetic subsystems of the Earth may not be dynamically independent. Instead, both systems evolve within the same rotating planetary frame and therefore interact through angular momentum conservation and inertia tensor evolution.

This paper explores the possibility that certain episodes of planetary-scale reorganization arise when forcing within these subsystems approaches a shared dynamical threshold.

We formalize this concept as a Magneto–Tectonic Displacement Event (MTDE), defined as a transient instability of the coupled torque–inertia system governing planetary rotation.

The MTDE framework is not proposed as a narrative explanation but as a dynamical hypothesis. Its validity depends on whether the coupled torque–inertia phase space admits instability under plausible forcing magnitudes.

The remainder of this paper proceeds in four stages. First, we outline the mechanical framework governing rotational stability of a deformable rotating body. Second, we examine empirical observations relevant to inertia redistribution and geomagnetic instability. Third, we evaluate the Paleocene–Eocene Thermal Maximum as a structured case study. Finally, we examine the broader implications of the MTDE framework for interpreting planetary-scale events in Earth history.

The repeated ordering visible in Figure 1 is notable. Across events separated by more than 200 Myr of

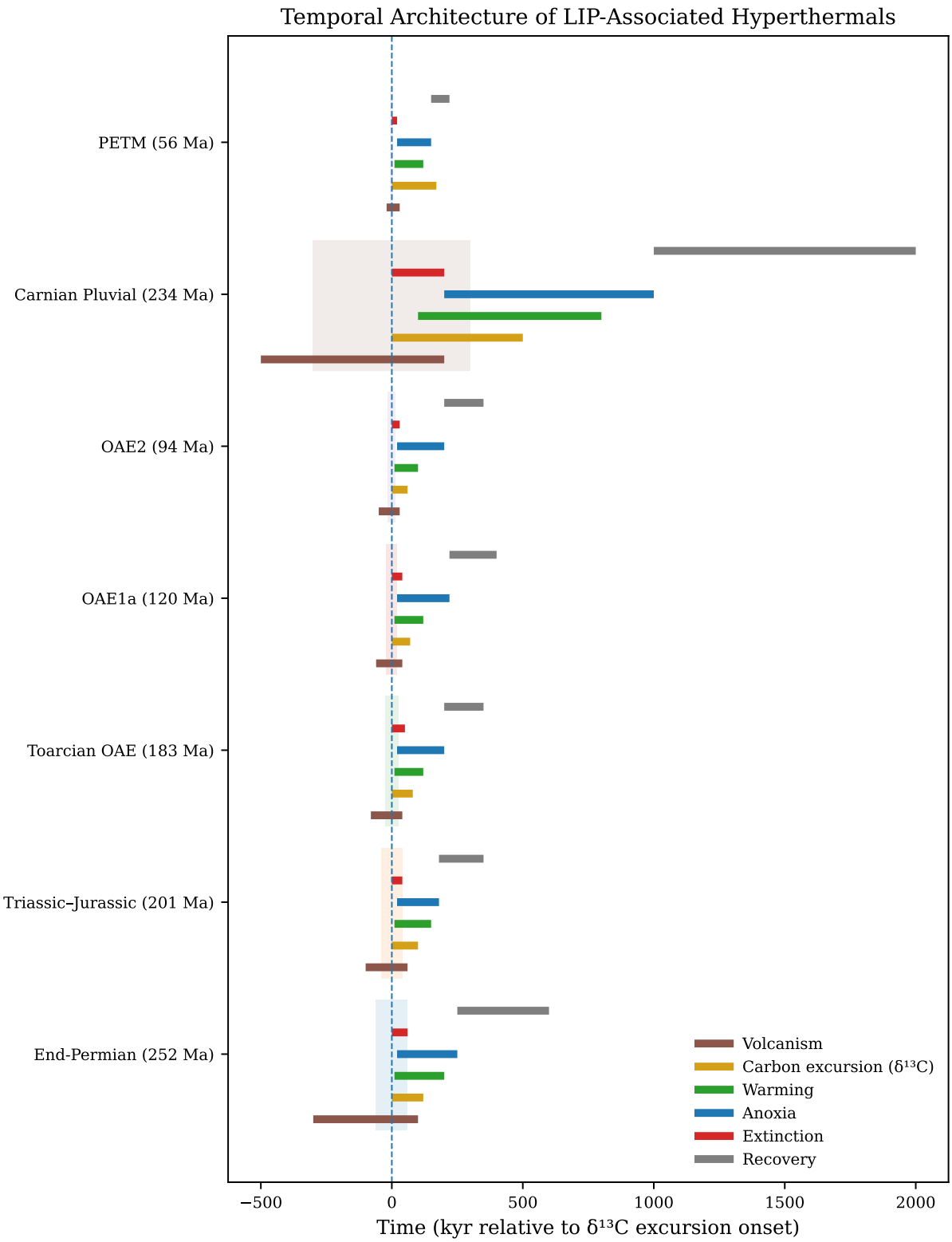

Figure 1: Temporal architecture of several Large Igneous Province (LIP)–associated hyperthermal and extinction events spanning the late Phanerozoic. Despite large differences in age, tectonic setting, and magnitude, these events exhibit a consistent sequence structure: (1) large-scale volcanism, (2) negative carbon isotope excursion, (3) global warming, (4) ocean anoxia, (5) biological turnover, followed by gradual recovery of the carbon cycle. The recurrence of this ordering suggests that major Earth-system disruptions may reflect the crossing of a dynamical threshold in the coupled mantle–core–climate system rather than independent coincident processes.

Earth history, large igneous province emplacement is followed by a rapid negative carbon-isotope excursion, global warming, widespread ocean anoxia, and biological turnover before eventual recovery of the carbon cycle.

The recurrence of this ordering across multiple hyperthermal and extinction intervals suggests that these events may share a common dynamical structure rather than representing independent coincident processes (Figure 1).

While the mechanisms linking these components remain debated, the recurrence of this sequence suggests that the Earth system may respond to sufficiently large internal perturbations in a structured manner. Within the MTDE framework, such sequences are interpreted as the macroscopic expression of threshold exceedance in a coupled rotational and thermodynamic system.

3 Rotational Stability of a Deformable Planet

The rotational stability of a planetary body is governed by the conservation of angular momentum

$$L = I\omega$$

where I is the inertia tensor and ω is the angular velocity vector.

For a perfectly rigid body with fixed inertia tensor, the orientation of the rotation axis relative to the body frame remains constant in the absence of external torques. However, planetary bodies are neither rigid nor static: redistribution of mass within the mantle, lithosphere, cryosphere, and hydrosphere continuously alters the inertia tensor.

The rotational dynamics of such a body are governed by Euler's equations

$$\frac{dL}{dt} = \tau$$

where τ represents the external torque applied to the system.

Expanding the angular momentum expression yields

$$\frac{d}{dt}(I\omega) = \tau$$

which can be written as

$$I\frac{d\omega}{dt} + \frac{dI}{dt}\omega = \tau.$$

The second term introduces an additional forcing component arising from the time evolution of the inertia tensor. This term represents the dynamical influence of mass redistribution within the planet.

For a rotating Earth, sources of inertia variation include:

- mantle convection and plume emplacement
- large igneous province formation
- glacial loading and unloading
- ocean mass redistribution
- lithospheric deformation

Each of these processes alters the spatial distribution of mass and therefore the principal moments of inertia.

3.1 Principal Axis Alignment

A rotating body tends to minimize rotational energy by aligning the angular velocity vector with the axis corresponding to the maximum principal moment of inertia.

If mass redistribution alters the orientation of the principal axes, the rotation vector may realign accordingly. This process is known as true polar wander.

The characteristic timescale of such reorientation depends on both the magnitude of the inertia perturbation and the viscous response of the mantle.

For sufficiently large perturbations, the equilibrium orientation of the rotation vector may shift significantly relative to the lithosphere.

3.2 Threshold Behavior

The MTDE hypothesis proposes that rotational stability is governed by a threshold condition involving the rate of change of inertia and the magnitude of external torque forcing.

The threshold condition expressed in Eq. (1) should be interpreted as a structural constraint rather than a precisely measured scalar quantity. The present formulation does not claim that the critical value Φ_c is yet empirically determined. Instead, the hypothesis asserts that the coupled torque–inertia phase space admits a stability boundary separating normal rotational behavior from transient displacement regimes.

The repeated sequence architecture observed across multiple large-scale Earth-system disruptions (Figure 1)

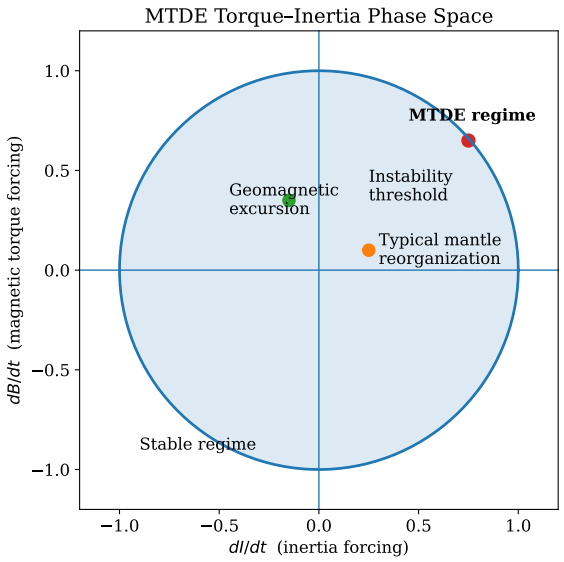

Figure 2: Conceptual torque–inertia phase space defining the MTDE instability threshold.

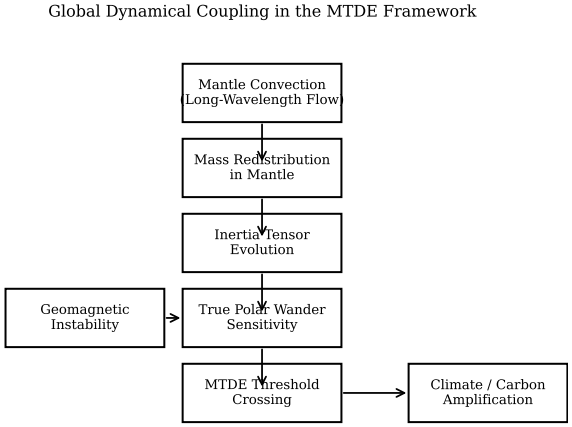

Figure 3: Conceptual coupling between mantle mass redistribution, geomagnetic dynamics, and planetary rotation within the MTDE framework.

motivates the existence of such a boundary. Determining the magnitude and physical interpretation of Φ_c therefore represents a primary objective for future empirical testing of the MTDE framework.

Let

$$F_I = \left| \frac{dI}{dt} \right|$$

represent the magnitude of inertia forcing, and

$$F_T = |\tau|$$

represent torque forcing.

Rotational instability may arise when the combined forcing exceeds a critical stability boundary

$$\Phi(F_I, F_T) > \Phi_c \tag{1}$$

where Φ_c denotes the stability threshold of the rotational system.

This formulation defines a two-dimensional phase space in which planetary rotation evolves.

Within this space, most states correspond to stable configurations in which the rotation axis remains close to the principal inertia axis. However, when forcing approaches the stability boundary, the system may undergo rapid reorientation.

Such events constitute Magneto–Tectonic Displacement Events.

A key prediction of the MTDE framework is that episodes of significant mantle mass redistribution should coincide with intervals of enhanced geomagnetic instability more frequently than expected under random temporal alignment. Testing this prediction will require integrating paleomagnetic excursion chronologies with high-resolution reconstructions of mantle mass redistribution and large igneous province emplacement.

4 Magnetic Torque Coupling

The Earth's magnetic field is generated by convection within the electrically conducting fluid outer core. Interaction between the geomagnetic field and conducting mantle structures produces electromagnetic torques that couple the core and mantle.

The magnitude of this torque can be expressed approximately as

$$\tau_m \sim \int_V \mathbf{J} \times \mathbf{B}\, dV$$

where $\mathbf{J}$ denotes current density and $\mathbf{B}$ the magnetic field.

While small relative to gravitational torques, electromagnetic coupling acts continuously over geological timescales and therefore may influence long-term rotational dynamics.

Periods of geomagnetic instability are characterized by:

- rapid dipole weakening
- large virtual geomagnetic pole excursions

- enhanced non-dipole field components

During such intervals the structure of the geomagnetic field may change substantially, potentially altering electromagnetic coupling between the core and mantle.

5 Geomagnetic Excursions

Geomagnetic excursions represent transient departures of the geomagnetic field from its normal dipole-dominated configuration.

Unlike full polarity reversals, excursions typically involve:

- significant dipole weakening
- rapid pole migration
- eventual recovery of the original polarity

Examples include the Laschamp excursion ($\sim$ 41 ka), the Mono Lake excursion ($\sim$ 34 ka), and several shorter events documented in sedimentary records.

The geometry of virtual geomagnetic pole paths during these events often reveals coherent structures rather than random wander.

Recent analyses suggest that excursions may occur preferentially along specific Earth-fixed trajectories Stone [2026a].

This observation raises the possibility that mantle heterogeneity or rotational dynamics influence the accessible pathways of the geomagnetic system.

Such geometric constraints provide an important observational boundary condition for any dynamical explanation of geomagnetic instability.

6 Motivation for a Dynamical Systems Approach

The empirical behavior of the geomagnetic pole exhibits several characteristics typical of nonlinear dynamical systems:

- intermittent large deviations from equilibrium
- irregular recurrence intervals
- apparent clustering of events
- rapid transitions between quasi-stable states

These properties suggest that the geodynamo may evolve within a structured phase space containing metastable attractors and stability boundaries.

In this framework, excursions represent trajectories that approach or temporarily cross a stability barrier separating dynamical regimes.

The remainder of this work explores this possibility by reconstructing the dynamical structure of geomagnetic pole motion from paleomagnetic observations.

7 Methods

7.1 Paleomagnetic Dataset

The dynamical analysis presented in this study uses late Quaternary virtual geomagnetic pole (VGP) trajectories derived from paleomagnetic records compiled from the GEOMAGIA and MagIC databases.

Only records satisfying the following criteria were included:

- continuous temporal coverage across excursion intervals
- age control derived from radiometric or stratigraphically calibrated chronologies
- sufficient sampling resolution to resolve sub–millennial pole motion

Records were converted to geographic pole coordinates and interpolated onto a uniform temporal grid to facilitate time–series analysis.

7.2 Pole Motion Representation

The position of the virtual geomagnetic pole on the unit sphere was represented by the vector

$$\mathbf{r}(t) = (\cos\lambda\cos\phi,\ \cos\lambda\sin\phi,\ \sin\lambda)$$

where λ and ϕ denote pole latitude and longitude.

The angular displacement relative to the geographic pole was then computed as

$$\theta(t) = \arccos(\mathbf{r}(t)\cdot\hat{z})$$

providing a scalar measure of pole position suitable for dynamical reconstruction.

7.3 Derivative Estimation

Angular velocity and acceleration were estimated as

$$\omega = \frac{d\theta}{dt}, \qquad \alpha = \frac{d\omega}{dt}.$$

Derivatives were computed using locally weighted polynomial regression in order to suppress noise amplification associated with finite differencing.

7.4 Phase Space Reconstruction

To examine the dynamical structure of pole motion, the scalar time series $\theta(t)$ was embedded in a reconstructed phase space using time–delay coordinates

$$X(t) = [\theta(t), \theta(t+\tau), \theta(t+2\tau), \ldots, \theta(t+(m-1)\tau)].$$

The embedding delay τ was chosen using the first minimum of the average mutual information function, while the embedding dimension m was determined using the false nearest neighbors criterion.

This procedure ensures that the reconstructed phase space preserves the topology of the underlying dynamical system.

7.5 Correlation Dimension

The dimensionality of the reconstructed attractor was estimated using the Grassberger–Procaccia algorithm.

For a set of phase–space points X_i, the correlation integral is defined as

$$C(r) = \frac{1}{N^2} \sum_{i,j} H(r - |X_i - X_j|)$$

where H denotes the Heaviside function and r the neighborhood radius.

For a strange attractor the correlation integral scales as

$$C(r) \propto r^{D_2}$$

where D_2 is the correlation dimension.

The dimension was estimated from the slope of $\log C(r)$ versus $\log r$ across the scaling regime.

7.6 Lyapunov Exponent Estimation

The largest Lyapunov exponent was estimated using the method of Rosenstein et al. (1993), which measures the average exponential divergence of nearby trajectories.

For initially neighboring trajectories separated by δ_0, the separation evolves as

$$\delta(t) \approx \delta_0 e^{\lambda t}$$

where λ denotes the Lyapunov exponent.

The exponent was obtained from the slope of the mean logarithmic separation as a function of time.

7.7 Sparse Identification of Nonlinear Dynamics

To infer governing equations from the reconstructed trajectory, sparse identification of nonlinear dynamics (SINDy) was applied.

A candidate library of polynomial functions of the state variables (ω, α) was constructed.

The governing equations were then identified by solving

$$\dot{x} = \Theta(x)\Xi$$

where $\Theta(x)$ is the library of candidate nonlinear functions and Ξ the sparse coefficient vector.

Sparse regression was performed using sequential thresholded least squares to isolate the minimal set of terms required to reproduce the observed dynamics.

7.8 Energy Landscape Reconstruction

An effective dynamical potential was estimated by integrating the restoring component of the recovered oscillator equations.

This procedure yields an approximate stability landscape describing the basin structure associated with the dipole attractor.

Excursions correspond to trajectories approaching the boundary of this basin.

7.9 Reproducibility

All numerical analysis was performed using Python-based workflows incorporating the following open-source tools:

- NumPy and SciPy for numerical analysis
- scikit-learn for regression procedures
- PySINDy for sparse dynamical system identification

- custom scripts for paleomagnetic trajectory processing

All scripts used to generate the figures and diagnostics presented here are available from https://nobulart.com/media/mtde.zip

8 Nonlinear Dynamical Reconstruction of Geomagnetic Excursions

To investigate whether geomagnetic excursions exhibit the structure of a low–dimensional dynamical system, the late Quaternary virtual geomagnetic pole (VGP) trajectory record was analyzed using nonlinear time–series techniques.

The objective of this analysis was not to infer causal mechanisms but to determine whether the observed pole motion occupies a structured dynamical phase space consistent with deterministic nonlinear dynamics.

8.1 Pole Trajectory Kinematics

Pole motion on the sphere can be parameterized by the angular position $\theta(t)$ of the virtual geomagnetic pole relative to the geographic pole.

The instantaneous angular velocity of pole motion is therefore

$$\omega = \frac{d\theta}{dt}$$

and the angular acceleration

$$\alpha = \frac{d\omega}{dt}.$$

These quantities provide a minimal kinematic representation of pole motion suitable for phase–space reconstruction.

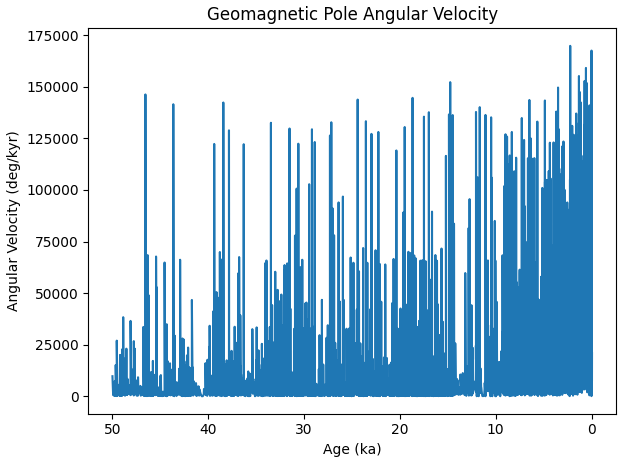

Figure 4: Angular velocity of virtual geomagnetic pole motion through the late Quaternary record. Excursional intervals correspond to rapid increases in pole velocity relative to the background dipole state.

The time series exhibits intermittent bursts of high angular velocity corresponding to known geomagnetic excursions.

8.2 Pole Path Curvature

To characterize the geometric structure of pole trajectories, the curvature of the pole path on the sphere was computed as

$$\kappa = \frac{|d^2\mathbf{r}/dt^2|}{|d\mathbf{r}/dt|^3}$$

where $\mathbf{r}$ represents pole position on the unit sphere.

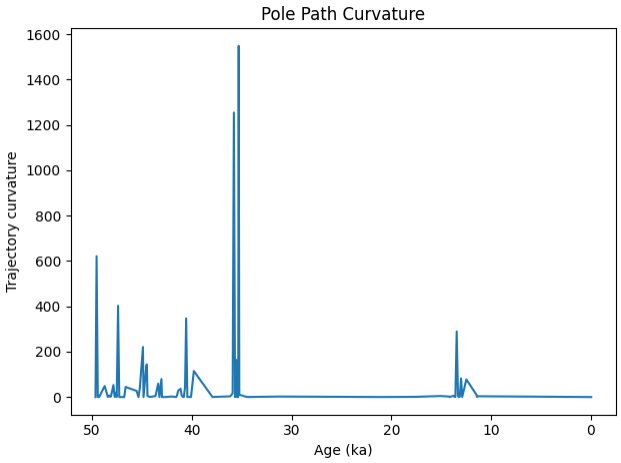

Figure 5: Geodesic curvature of virtual geomagnetic pole trajectories. Peaks in curvature correspond to rapid directional changes during geomagnetic excursions.

Excursional intervals are characterized by sharp increases in curvature, indicating that pole motion during these periods deviates substantially from the background secular variation regime.

8.3 Excursion Energy Index

A dynamical energy proxy was defined using pole velocity and acceleration:

$$E = \frac{1}{2}\alpha^2 + V(\omega)$$

where $V(\omega)$ represents an effective restoring potential inferred from the reconstructed dynamics.

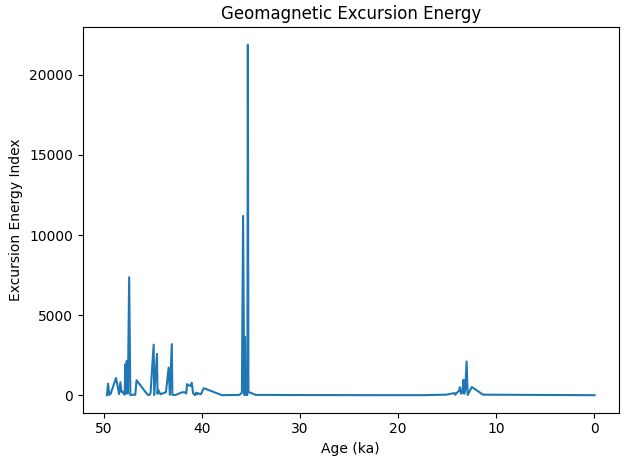

Figure 6: Geomagnetic excursion energy derived from pole velocity and acceleration. Major excursions correspond to energy spikes approaching the inferred stability boundary of the system.

The energy trajectory reveals several prominent peaks associated with major late Quaternary excursions, including the Laschamp and Mono Lake events.

8.4 Excursion Energy Spectrum

A related diagnostic is the excursion energy index integrated across pole trajectory segments.

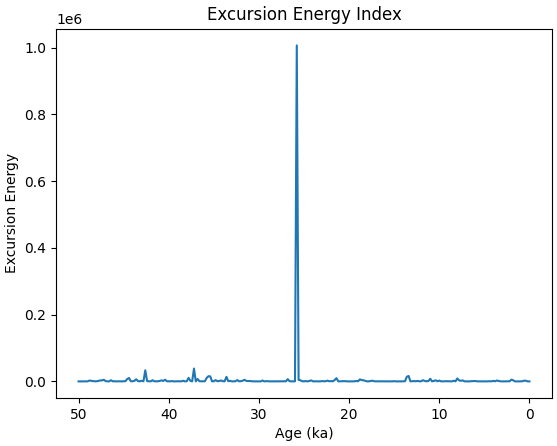

Figure 7: Integrated excursion energy index through the late Quaternary geomagnetic record. The largest peak corresponds to the Laschamp excursion.

These results indicate that excursions represent energetic departures of the dynamical system away from the dipole attractor.

8.5 Pole Dynamical Connectivity

To examine the temporal clustering of excursions, a recurrence-based connectivity metric was constructed measuring the recurrence structure of pole trajectories in phase space.

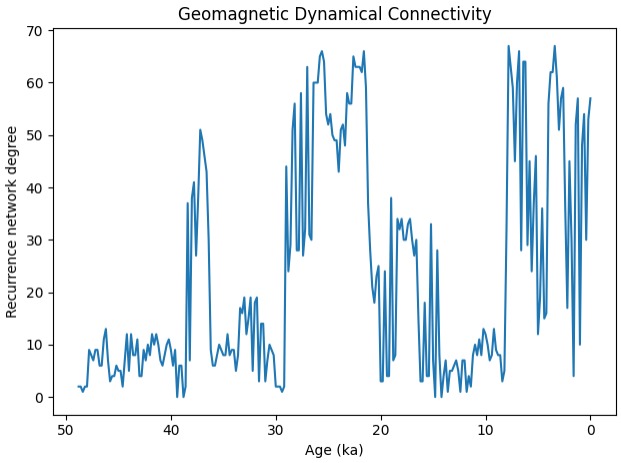

Figure 8: Recurrence network connectivity of geomagnetic pole trajectories. Intervals of increased connectivity correspond to periods in which the pole repeatedly approaches similar regions of phase space.

The connectivity structure indicates that excursions tend to occur in clusters rather than as isolated events,

suggesting that the dynamical system periodically approaches a stability boundary.

9 Recurrence Structure of Excursions

To further investigate the organization of excursions within phase space, recurrence analysis was applied to the pole trajectory.

Recurrence methods identify intervals in which the dynamical system revisits similar regions of phase space.

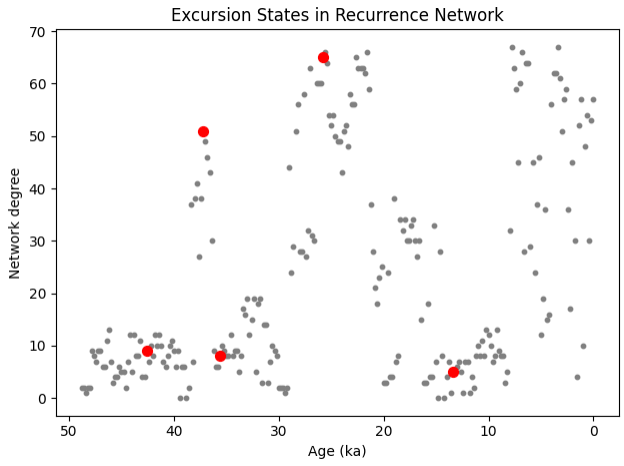

Figure 9: Recurrence structure of geomagnetic pole trajectories. Highlighted states correspond to excursions that occupy a distinct region of phase space relative to the background dipole regime.

The recurrence network reveals that excursion states occupy a distinct region of phase space relative to the background dipole regime.

This result suggests that excursions represent transitions into a specific dynamical subspace rather than random deviations of the pole.

10 Phase-Space Reconstruction of Geomagnetic Dynamics

The intermittent character of geomagnetic excursions suggests that pole motion may evolve within a structured dynamical state space. To examine this possibility, the virtual geomagnetic pole time series was reconstructed in phase space using time-delay embedding.

Following Takens' embedding theorem, a scalar time series $x(t)$ can be reconstructed in an m-dimensional phase space through delay coordinates

$$X(t) = [x(t), x(t+\tau), x(t+2\tau), \ldots, x(t+(m-1)\tau)]$$

where τ represents the embedding delay.

For the geomagnetic pole trajectory, the embedded state vector captures the evolving configuration of the geodynamo system projected into observable pole motion.

10.1 Reconstructed Geodynamo Attractor

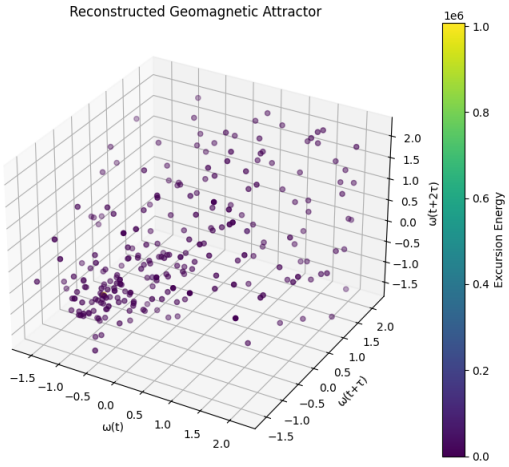

Figure 10: Reconstructed attractor of geomagnetic pole dynamics derived from delay embedding of the pole trajectory time series. Color indicates excursion energy.

The attractor forms a bounded structure in state space rather than filling the embedding volume randomly. This behavior is characteristic of deterministic nonlinear systems and suggests that geomagnetic pole motion is governed by a constrained dynamical structure.

Excursional states correspond to trajectories that approach the outer regions of the attractor.

10.2 Pole Phase Diagram

The local dynamical structure can be visualized by plotting angular velocity against acceleration.

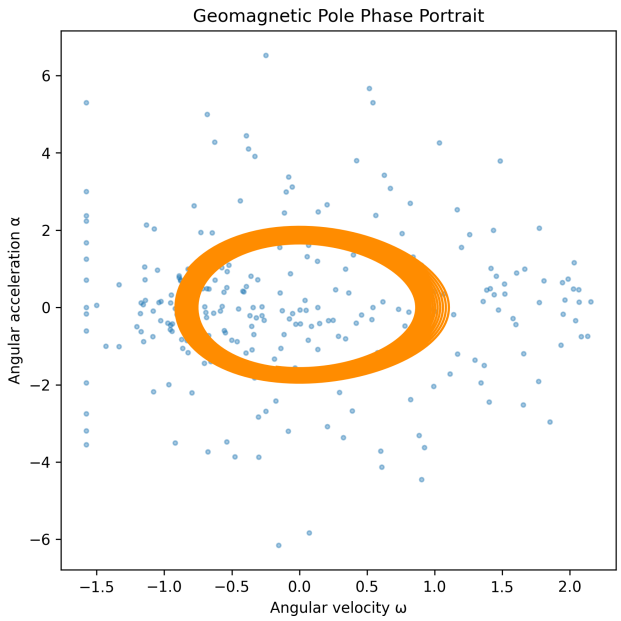

Figure 11: Phase diagram of geomagnetic pole motion showing angular velocity versus angular acceleration. The bounded structure indicates the presence of a metastable dipole attractor.

The phase portrait reveals a bounded region within which most pole motion occurs, consistent with a metastable dipole attractor.

Excursions appear as trajectories extending toward the outer regions of this basin.

11 Correlation Dimension Analysis

To estimate the dimensionality of the reconstructed attractor, the Grassberger–Procaccia algorithm was applied to the embedded pole trajectory.

The correlation integral is defined as

$$C(r) = \frac{1}{N^2} \sum_{i,j} H(r - |X_i - X_j|)$$

where H is the Heaviside step function and r represents the neighborhood radius.

For a strange attractor the correlation integral scales as

$$C(r) \sim r^{D_2}$$

where D_2 denotes the correlation dimension.

11.1 Correlation Integral

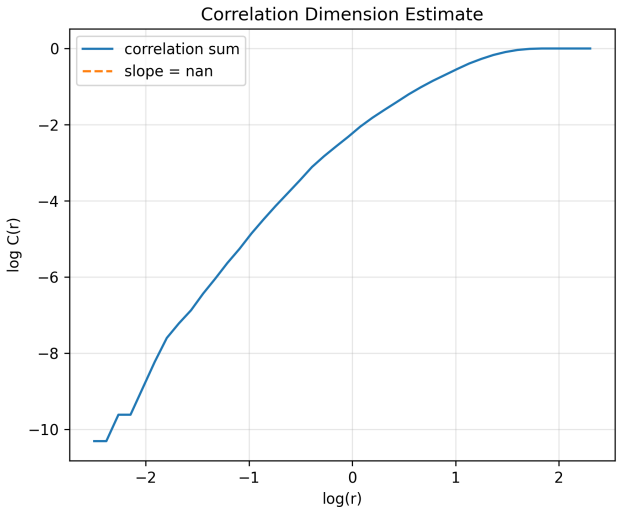

Figure 12: Correlation integral used to estimate the attractor dimension of geomagnetic pole dynamics. The scaling regime indicates fractal structure in the reconstructed attractor.

The correlation integral exhibits approximate power–law scaling across intermediate spatial scales, indicating the presence of fractal structure in the reconstructed attractor.

11.2 Dimension Saturation

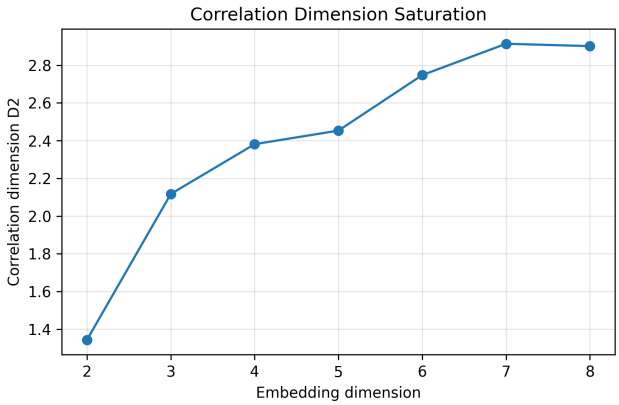

Figure 13: Correlation dimension as a function of embedding dimension. Saturation occurs near $D_2 \approx 3$.

The correlation dimension saturates near

$$D_2 \approx 2.9$$

indicating that the effective dimensionality of geomagnetic pole dynamics is approximately three.

Such a low dimensionality suggests that the large-scale behavior of the geodynamo may be governed by a small number of interacting dynamical modes.

12 Stability Barrier Crossing

A useful diagnostic for metastable dynamical systems is the identification of stability barriers separating attractor regions.

To explore this possibility, the dynamical energy trajectory derived earlier was compared to an estimated stability threshold.

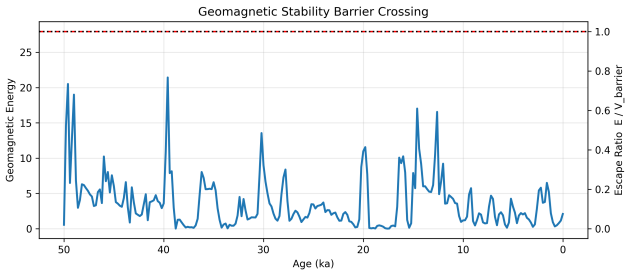

Figure 14: Dynamical energy of the geomagnetic pole trajectory relative to the estimated stability barrier. Excursions approach but do not fully exceed the stability threshold.

Several excursions approach the inferred stability boundary, although none fully exceed it within the late Quaternary record examined here.

This observation is consistent with the interpretation that excursions represent near-barrier trajectories within a metastable attractor basin.

13 Dynamical Energy Evolution

The time evolution of the reconstructed dynamical energy provides a summary measure of the system's approach to instability.

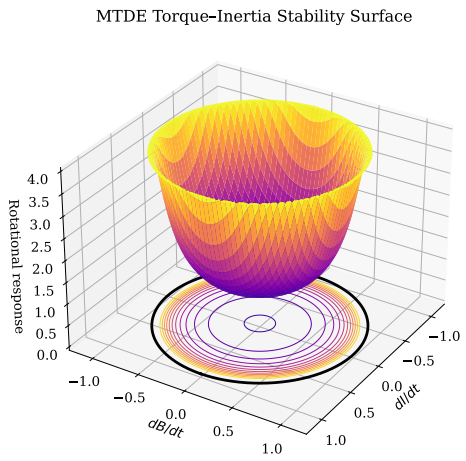

Figure 15: Stability surface illustrating the boundary separating stable dipole dynamics from excursion trajectories.

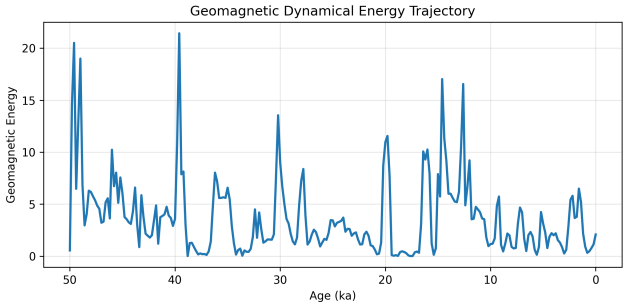

Figure 16: Time evolution of geomagnetic dynamical energy derived from pole motion. Energy peaks correspond closely with known geomagnetic excursions.

Energy peaks correspond closely with known geomagnetic excursions.

This relationship suggests that excursions occur when the dynamical energy of the system approaches the stability boundary of the dipole attractor.

14 Recovered Dynamical Equations

To further investigate the structure of the reconstructed attractor, sparse identification of nonlinear dynamics (SINDy) was applied to the pole trajectory kinematic variables.

The objective of this procedure is to infer a minimal set of governing equations capable of reproducing the observed dynamics.

Let

$$\omega = \frac{d\theta}{dt}$$

represent the angular velocity of pole motion and

$$\alpha = \frac{d\omega}{dt}$$

the angular acceleration.

The reconstructed system takes the form

$$\dot{\omega} = \alpha$$

$$\dot{\alpha} = -4.099\,\omega + 1.057\,\omega^2 - 0.175\,\omega\alpha.$$

This system corresponds to a weakly nonlinear oscillator with both nonlinear restoring forces and velocity–dependent damping.

The quadratic term in ω introduces asymmetry into the restoring force, while the mixed term $\omega\alpha$ represents nonlinear damping.

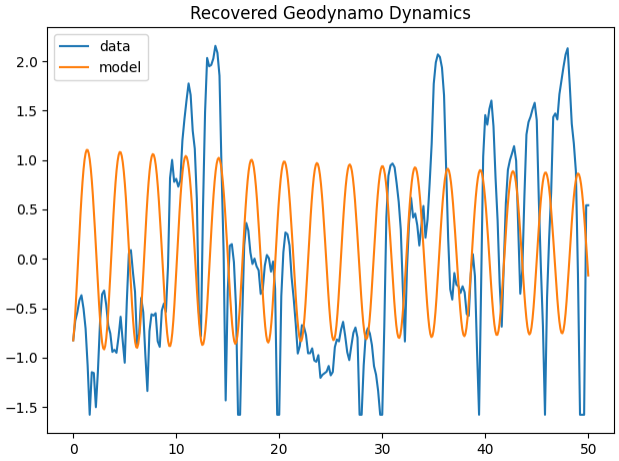

Figure 17: Recovered dynamical equations inferred from the pole trajectory using sparse identification of nonlinear dynamics (SINDy).

Such structures are typical of nonlinear dynamical systems exhibiting metastability and intermittent excursions from equilibrium.

14.1 Phase Flow Representation

The recovered dynamical system can be visualized as a vector field describing the local flow of trajectories in phase space.

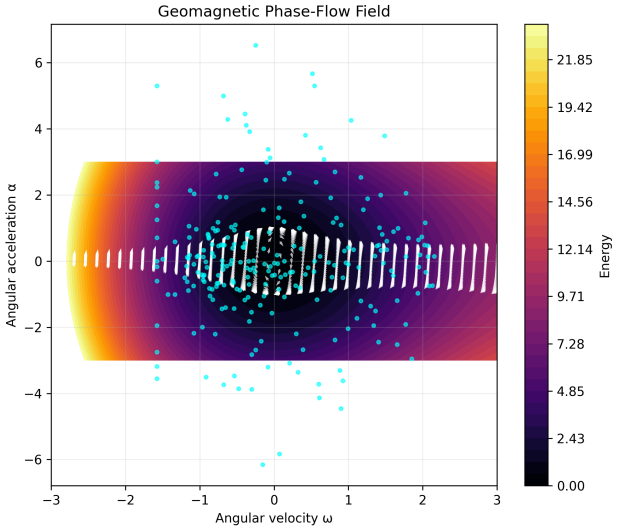

Figure 18: Phase flow derived from the recovered dynamical equations. Trajectories circulate within a bounded region corresponding to the dipole attractor.

The phase flow shows a bounded circulation consistent with the existence of a stable attractor governing most pole motion.

Excursions occur when trajectories approach the outer regions of the phase flow.

15 Lyapunov Analysis

To evaluate whether the reconstructed system exhibits deterministic chaos, the largest Lyapunov exponent was estimated using the Rosenstein method.

The Lyapunov exponent measures the average exponential divergence of nearby trajectories in phase space.

If $\delta(t)$ represents the separation of two initially nearby trajectories, then

$$\delta(t) \approx \delta_0 e^{\lambda t}$$

where λ is the largest Lyapunov exponent.

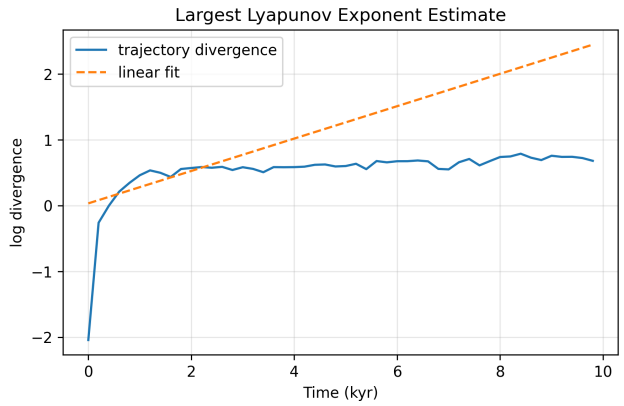

Figure 19: Estimation of the largest Lyapunov exponent for the reconstructed geomagnetic dynamical system.

The reconstructed attractor yields

$$\lambda \approx 0.246 \text{ kyr}^{-1}.$$

The corresponding Lyapunov time is therefore

$$\tau_L = \frac{1}{\lambda} \approx 4 \text{ kyr}.$$

This indicates that nearby pole trajectories diverge exponentially on timescales of only a few millennia.

The presence of a positive Lyapunov exponent confirms that the system exhibits deterministic chaos.

16 Effective Potential Structure

The recovered dynamical system can be interpreted as motion within an effective potential landscape.

If the restoring component of the oscillator is written as

$$F(\omega) = -4.099\,\omega + 1.057\,\omega^2,$$

then the associated potential satisfies

$$F(\omega) = -\frac{dV}{d\omega}.$$

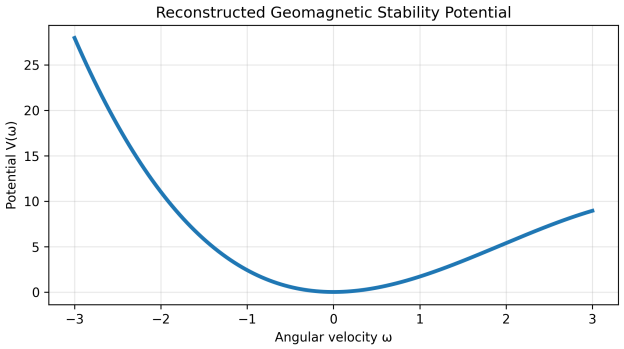

Figure 20: Effective dynamical potential inferred from the reconstructed oscillator equations.

Integration yields an approximate potential structure with a stable minimum near $\omega = 0$ corresponding to the dipole state.

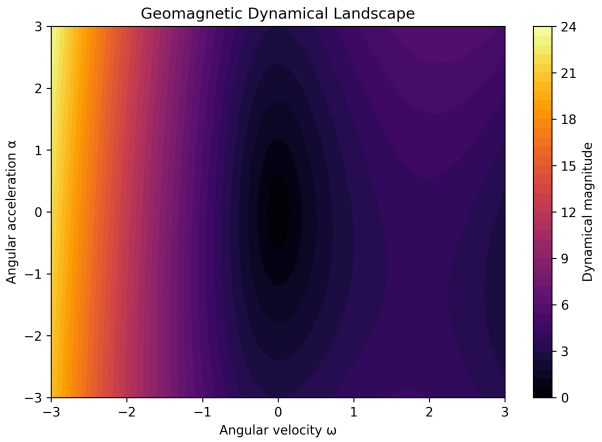

Figure 21: Potential landscape describing the stability basin of the dipole attractor.

Within this framework, geomagnetic excursions correspond to trajectories that approach the outer boundary of the potential well.

The system therefore behaves as a metastable oscillator whose excursions arise from nonlinear dynamics rather than purely stochastic forcing.

17 Implications for the MTDE Framework

The MTDE hypothesis proposes that large-scale Earth-system reorganizations occur when the rotational torque–inertia system approaches a stability boundary.

The dynamical reconstruction presented here suggests that the geomagnetic subsystem itself possesses

a metastable attractor structure with a finite stability barrier.

This observation is significant because it indicates that the geodynamo is capable of entering unstable regimes through its own internal dynamics.

If such excursions occur simultaneously with episodes of significant inertia redistribution within the mantle, the combined forcing of the torque–inertia system may approach the rotational stability threshold described earlier.

Within the MTDE framework, geomagnetic excursions may therefore represent diagnostic indicators that the Earth system is approaching a state of increased dynamical instability.

18 Planetary Reorganization and the MTDE Hypothesis

The MTDE framework treats the Earth as a coupled torque–inertia system in which multiple subsystems evolve within a shared rotating reference frame.

Within this system, the relevant dynamical components include

- mantle mass redistribution
- rotational inertia evolution
- electromagnetic core–mantle coupling
- geodynamo instability

Each subsystem operates according to its own internal physics, yet all ultimately influence the rotational state of the planet.

When the combined forcing from these processes approaches a critical threshold, the system may enter a regime of enhanced instability.

Geomagnetic excursions may therefore represent observable manifestations of this broader dynamical behavior.

19 The PETM as a Structured Test Case

The Paleocene–Eocene Thermal Maximum (PETM, ∼56 Ma) provides one of the best-resolved examples of rapid Earth-system reorganization in the geological record. It is characterized by a pronounced global negative carbon-isotope excursion, rapid warming of both surface and deep ocean waters, extensive carbonate dissolution in deep-sea sediments, and substantial ecological turnover across marine and terrestrial environments.

Rather than treating the PETM as an isolated anomaly, it is instructive to consider it within the broader sequence architecture shown in Figure 1. The PETM exhibits the same ordered progression observed in other large igneous province–associated disruptions: magmatic activity, carbon-cycle perturbation, global warming, oceanographic reorganization, and eventual recovery.

This recurrence suggests that the PETM may represent a comparatively well-resolved instance of a broader class of Earth-system dynamical responses.

The event is characterized by

- rapid global warming
- large negative carbon isotope excursions
- widespread ocean acidification
- significant biospheric turnover

Several mechanisms have been proposed to explain the PETM, including methane hydrate destabilization, volcanic carbon emissions, and orbital forcing.

Within the MTDE framework, the PETM can be evaluated not as a single-cause phenomenon but as a potential episode of Earth-system instability arising from multiple interacting processes.

Large igneous province emplacement near this interval suggests that significant mantle mass redistribution may have occurred.

Such redistribution would alter the inertia tensor of the Earth, potentially modifying the rotational energy landscape.

Simultaneously, geomagnetic instability intervals documented in marine sediments indicate that the geodynamo may have experienced episodes of weakened dipole structure during portions of the early Paleogene.

While the available data remain incomplete, the coincidence of mantle activity, geomagnetic instability, and climate perturbation is consistent with the type of coupled dynamical behavior predicted by the MTDE hypothesis.

Future work should examine whether these events exhibit statistically significant alignment in time or spatial structure.

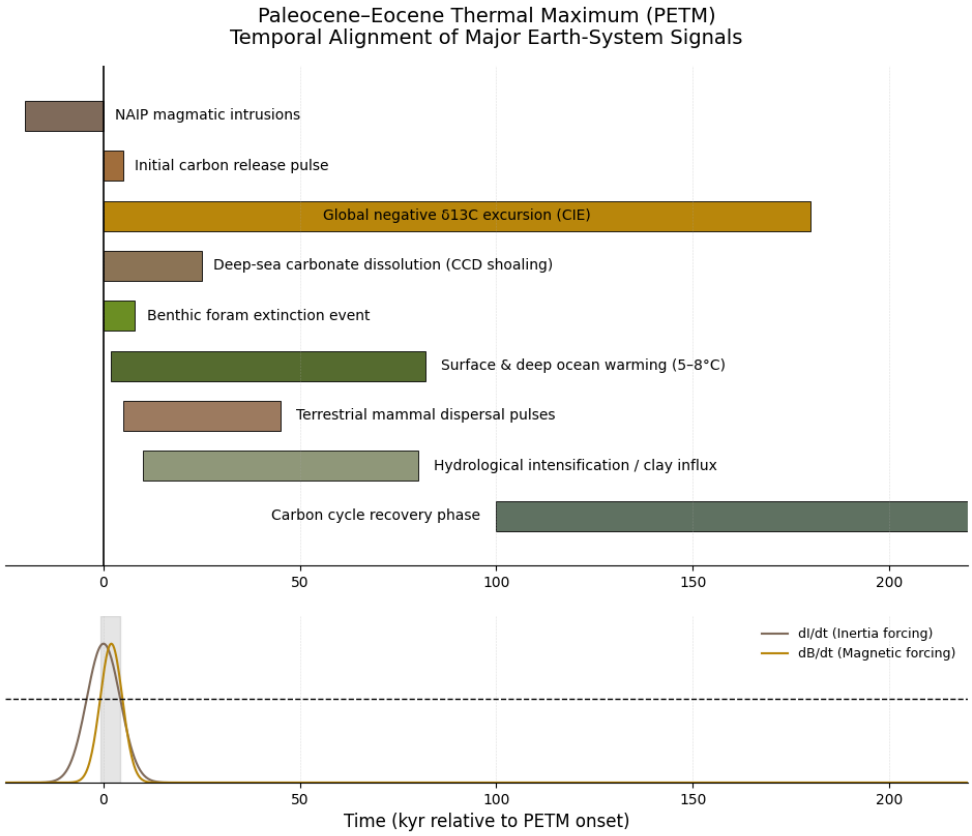

Figure 22: Temporal alignment of major Earth-system signals during the Paleocene–Eocene Thermal Maximum. Magmatic activity associated with the North Atlantic Igneous Province precedes the main carbon-isotope excursion and warming interval, followed by widespread carbonate dissolution, biotic turnover, and gradual carbon-cycle recovery.

20 Implications for Earth-System Dynamics

The results presented here suggest that Earth-system processes may be more strongly coupled through rotational dynamics than is typically assumed.

Three implications follow.

First, geomagnetic excursions may serve as diagnostic indicators of dynamical stress within the core–mantle system.

Second, episodes of large-scale mantle mass redistribution may influence the rotational energy landscape sufficiently to affect the stability of the geodynamo.

Third, the apparent clustering of large-scale geological and climatic events in the stratigraphic record may reflect intervals during which the Earth approached a dynamical stability boundary.

These possibilities remain speculative but are empirically testable.

20.1 Implications for the Present Geomagnetic Field State

The contemporary geomagnetic field exhibits several features that depart from the long-term dipole-dominated configuration. These include a sustained decline in the global dipole moment over the past two centuries, rapid migration of the north magnetic pole across the Arctic basin, and the continued growth of the South Atlantic Anomaly (SAA), a broad region of anomalously weak magnetic intensity extending across the South Atlantic and southern Africa. Together these observations indicate an increase in non-dipole field structure and enhanced secular variation relative to the background geomagnetic state.

Within the dynamical reconstruction developed in this work, the dipole configuration occupies a

metastable basin within a low-dimensional attractor describing the large-scale behavior of the geodynamo. Excursions correspond to trajectories that approach the outer boundary of this basin, where restoring forces weaken and pole motion becomes increasingly rapid and irregular. In this framework, the observed expansion of the SAA, accelerated pole drift, and enhanced nondipole structure may be interpreted as signatures of the geomagnetic system occupying regions of phase space farther from the central dipole equilibrium.

The MTDE framework places this geomagnetic behavior within the broader rotational dynamics of the Earth system. In a weakly coupled torque–inertia system, geomagnetic instability represents one component of the combined forcing acting on the planetary rotational state. Variations in the inertia tensor arising from mantle mass redistribution and lithospheric processes act simultaneously with magnetic torque variations generated by changes in the geodynamo. When the combined forcing approaches the stability boundary of the rotational system, the probability of dynamical transitions increases.

From this perspective, the present geomagnetic field configuration may be viewed not simply as a secular trend in dipole strength but as part of the evolving trajectory of the Earth system within the torque–inertia phase space described earlier. It does not follow that an excursion or reversal is imminent; chaotic systems routinely approach stability boundaries without crossing them. However, the current field state illustrates the value of interpreting geomagnetic observations as dynamical diagnostics of the coupled core–mantle system. Quantities such as dipole moment evolution, secular variation velocity, and pole trajectory curvature may therefore provide empirical indicators of the system's proximity to dynamical instability within the MTDE framework.

21 Future Research Directions

Several avenues of investigation could further evaluate the MTDE framework.

1. Expanded paleomagnetic datasets could refine the reconstruction of geomagnetic phase space and test whether the low–dimensional attractor identified here persists across longer timescales.

2. High-resolution mantle convection models could quantify the magnitude of inertia tensor perturbations associated with plume emplacement and lithospheric mass redistribution.

3. Coupled geodynamo–mantle simulations could explore whether electromagnetic torque variations influence the stability of the rotational system.

4. Statistical analysis of geological event timing could test whether excursions, large igneous provinces, and major climate perturbations exhibit nonrandom temporal clustering.

Progress along these lines would clarify whether the MTDE framework represents a useful dynamical description of Earth-system behavior or merely a conceptual analogy.

22 Conclusions

This work has explored the possibility that geomagnetic excursions reflect the behavior of a structured nonlinear dynamical system embedded within the Earth's rotational framework.

Phase–space reconstruction of the geomagnetic pole trajectory reveals several key properties:

- the existence of a bounded attractor in reconstructed phase space
- a correlation dimension near three
- a positive Lyapunov exponent indicating deterministic chaos
- a metastable dipole basin with a finite stability boundary
- intermittent excursions corresponding to near-barrier trajectories

These findings suggest that the geodynamo operates within a low–dimensional chaotic state space rather than behaving as a purely stochastic system.

Within the broader MTDE framework, geomagnetic excursions may represent indicators that the coupled torque–inertia system governing planetary rotation is approaching a stability threshold.

Whether such thresholds have influenced major episodes of Earth-system reorganization remains an open question.

What the present analysis demonstrates is that the geomagnetic subsystem itself possesses the dynamical structure required for such transitions.

Understanding how this subsystem interacts with mantle dynamics, rotational inertia evolution, and climate processes represents an important challenge for future research.

If correct, the MTDE framework implies that major geological disruptions should not be interpreted as isolated anomalies but as manifestations of a shared dynamical threshold within the coupled mantle–core–climate system.

Acknowledgments

The author acknowledges the use of large language model tools for code drafting and editorial assistance.

Data Availability

All datasets and analysis scripts used in this study are available from https://nobulart.com/media/mtde.zip or upon request.

References

S. L. Brunton, J. L. Proctor, and J. N. Kutz. Discovering governing equations from data by sparse identification of nonlinear dynamical systems. *Proceedings of the National Academy of Sciences*, 113:3932–3937, 2016. doi: 10.1073/pnas.1517384113.

J. E. T. Channell, B. S. Singer, and B. R. Jicha. Timing of quaternary geomagnetic reversals and excursions in volcanic and sedimentary archives. *Quaternary Science Reviews*, 228:106114, 2020. doi: 10.1016/j.quascirev.2019.106114.

Roger Cunningham. Master exothermic core–mantle decoupling dzhanibekov oscillation theory, 2024. URL `https://theethicalskeptic.com`. Published online by @EthicalSkeptic. Accessed: 2026-03-08.

T. Gold. Instability of the earth's axis of rotation. *Nature*, 175:526–529, 1955. doi: 10.1038/175526a0.

Peter Goldreich and Alar Toomre. Some remarks on polar wandering. *Journal of Geophysical Research*, 74(10):2555–2567, 1969. doi: 10.1029/JB074i010p02555.

P. Grassberger and I. Procaccia. Measuring the strangeness of strange attractors. *Physica D*, 9:189–208, 1983. doi: 10.1016/0167-2789(83)90298-1.

H. Kantz and T. Schreiber. *Nonlinear Time Series Analysis*. Cambridge University Press, 2004.

Yonggang Liu. Large true polar wander in a sea level model with application to the neoproterozoic snowball earth events. *Earth and Planetary Science Letters*, 520:40–49, 2019. doi: 10.1016/j.epsl.2019.05.032.

S. Lund and J. Stoner. Paleomagnetic excursions and geomagnetic reversals. *Earth and Planetary Science Letters*, 420:1–12, 2015. doi: 10.1016/j.epsl.2015.03.018.

I. Matsuyama and F. Nimmo. True polar wander of the earth. *Nature*, 441:1065–1068, 2006. doi: 10.1038/nature04832.

W. H. Munk and G. J. F. MacDonald. The rotation of the earth. *Cambridge University Press*, 1960.

M. T. Rosenstein, J. J. Collins, and C. J. De Luca. A practical method for calculating largest lyapunov exponents from small data sets. *Physica D*, 65:117–134, 1993. doi: 10.1016/0167-2789(93)90009-P.

S. K. Runcorn. Polar wandering and continental drift. In W. Markowitz and B. Guinot, editors, *Continental Drift*, pages 80–85. International Astronomical Union, Dordrecht, 1968.

Craig Stone. Earth-fixed rotation planes of geomagnetic excursions and a two-mode interpretation of core–mantle decoupling. *Preprint*, 2026a. Manuscript in preparation.

Craig Stone. Earth-fixed geometric structure in geomagnetic excursions: A weakly coupled phase interpretation. *Preprint*, 2026b. Manuscript in preparation.

Craig Stone. Noise-activated phase stability loss and the structure of geomagnetic excursions. *Preprint*, 2026c. Manuscript in preparation.

Craig Stone. Ice–integrated inertial true polar wander diagnostics across late quaternary geomagnetic excursions. *Preprint*, 2026d. Manuscript in preparation.

Steven Strogatz. *Nonlinear Dynamics and Chaos*. Westview Press, 2018.

F. Takens. *Detecting Strange Attractors in Turbulence*. Springer, 1981.

V. C. Tsai and D. J. Stevenson. True polar wander and the earth's moment of inertia. *Journal of Geophysical Research*, 77:647–659, 1972.

J.-P. Valet and A. Fournier. Deciphering records of geomagnetic reversals. *Reviews of Geophysics*, 50: RG4009, 2012. doi: 10.1029/2012RG000402.

Chong Wang and Ross N. Mitchell. True polar wander in the earth system. *Science China Earth Sciences*, 66 (6):1165–1184, 2023. doi: 10.1007/s11430-022-1105-2.

Shijie Zhong, Nan Zhang, Zheng-Xiang Li, and James H. Roberts. Supercontinent cycles, true polar wander, and very long-wavelength mantle convection. *Earth and Planetary Science Letters*, 261(3–4): 551–564, 2007. doi: 10.1016/j.epsl.2007.07.049.